Advances in Concrete Construction, *Vol. 3, No. 4 (2015) 283-293*
DOI: http://dx.doi.org/10.12989/acc.2015.3.4.283

Compressive strength and failure behaviour of fibre reinforced concrete at elevated temperatures

F.U.A. Shaikh* and M. Taweel

Department of Civil Engineering, Curtin University, Perth, Australia

(Received July 20, 2015, Revised December 10, 2015, Accepted December 23, 2015)

Abstract. This paper presents the effects of elevated temperatures of 400°C and 800°C on the residual compressive strength and failure behaviour of fibre reinforced concretes and comparison is made with that of unreinforced control concrete. Two types of short fibres are used in this study e.g., steel and basalt fibres. The results show that the residual compressive strength capacity of steel fibre reinforced concrete is higher than unreinforced concrete at both elevated temperatures. The basalt fibre reinforced concrete, on the other hand, showed lower strength retention capacity than the control unreinforced concrete. However, the use of hybrid steel-basalt fibre reinforcement recovered the deficiency of basalt fibre reinforced concrete, but still slightly lower than the control and steel fibres reinforced concretes. The use of fibres reduces the spalling and explosive failure of steel, basalt and hybrid steel-basalt fibres reinforced concretes oppose to spalling in deeper regions of ordinary control concrete after exposure to above elevated temperatures. Microscopic observation of steel and basalt fibres surfaces after exposure to above elevated temperatures shows peeling of thin layer from steel surface at 800°C, whereas in the case of basalt fibre formation of Plagioclase mineral crystals on the surface are observed at elevated temperatures.

Keywords: concrete; fibres,; elevated temperatures,;fire; compressive strength; failure behaviour

1. Introduction

Concrete is the most widely used construction material due to its low cost, easy constructability, better mechanical and durability, etc.. During service life, the reinforced concrete (RC) structures experience various extreme events e.g., high wind pressure during cyclone, different chemical exposures, dynamic forces due to earthquake and accidental blast and impact, etc. RC structures seldom experience fire during their life time. However, during fire, the RC is severely damaged and often shows severe spalling damage and significant loss of mechanical properties. The loss of mechanical strength at elevated temperatures is attributed to the formation of cracks and spalling of concrete due to deterioration of cement paste and its bond with aggregate. At elevated temperatures, the pore water as well as chemically bound water in cement paste evaporate and form internal pore pressure, which often causes cracking of cement paste and damage its bond with aggregates, results in spalling of concrete. A common technique to reduce

*Corresponding author, Ph.D., E-mail: s.ahmed@curtin.edu.au

Copyright © 2015 Techno-Press, Ltd.
http://www.techno-press.org/?journal=acc&subpage=7 ISSN: 2234-0912 (Print), 2234-179X (Online)

the internal pressure inside the concrete during fire is the addition of short polymeric fibres, which melts at relatively low temperature (generally below 250-300°C) and creates additional voids to release the internal pressure (Wetzig 2002, Ali *et al*. 1996).

Fibre reinforced concrete (FRC) has been steadily developed over the last few decades. The primary reason of addition of fibres is to improve the tensile and flexural strength of concrete and also to improve the post-cracking ductility of concrete. Various types of fibres are used to reinforced the concrete. While polymeric FRC shows spalling resistance at fire, however, its post fire residual mechanical properties is of great concern, as these fibres are melt at elevated temperatures or lose their properties significantly if not melted. In addition to polymeric fibres, steel fibres are also widely used to reinforce concrete. Recently, basalt fibre, which is manufactured from natural basalt rock, is also used in cement composite. The advantage of steel and basalt fibres reinforced FRC at elevated temperatures during fire is their inherent higher melting temperature than the polymeric fibres. A number of studies are reported on the effect of elevated temperatures on mechanical properties and failure behaviour of steel FRC. Poon *et al*. (2004) evaluated the effects of elevated temperatures of 600 and 800°C on the compressive strength of steel and polyproplylene (PP) FRC. It is reported that the residual compressive strengths of steel FRC and PP FRC are about 50% and 55% of original, respectively after exposure to 600°C. At 800°C the residual compressive strengths are 25% and 33% for steel FRC and PP FRC, respectively. Chen and Liu (2004) have also reported a similar study but in high strength concrete. They have reported that the residual compressive strengths of steel FRC are about 90%, 60% and 38% of the original at 400, 600 and 800°C, respectively, where as in the case of PP FRC these values are about 52%, 50% and 30%, respectively. The authors also measured the residual tensile strengths (splitting) of above FRCs and observed similar reduction. In another study, Suhaendi and Horiguchi (2006) also reported similar rate of reduction in the compressive and tensile strengths of both steel and PP FRC at 200 and 400°C. In a recent study on steel FRC, Dugenci *et al*. (2015) reported about 78% to 96% reduction in the compressive strength of steel FRC at 900 to 1200°C temperatures. Kim *et al*. (2015) in their recent study also reported reductions in the compressive strengths of the steel FRC at elevated temperatures. While considerable research has been conducted on the effect of elevated temperatures on mechanical properties of steel and PP FRCs, no such study is so far reported on the basalt FRC. Due to higher fire resistance of basalt fibre than steel and PP fibres, the basalt FRC is expected to behave better than its counterpart steel FRC. This paper presents the comparative behaviour of steel and basalt FRC after exposure to elevated temperatures of 400 and 800^{o}C. The hybrid effect of steel and basalt fibres is also evaluated by comparing the steel and basalt FRC with hybrid steel-basalt FRC. Residual compressive strength and failure behaviour of above concretes at elevated temperatures are measured. In addition the microstructural changes of steel and basalt fibres after exposure to above elevated temperatures are also studies through scanning electron microscope analysis.

2. Materials and mix proportions

Ordinary Portland cement (OPC) was used to cast all concretes in this study. Granite rocks of 10 mm and 20 mm sizes were used as coarse aggregates, while the river sand was used as the fine aggregate. The steel fibre was hooked end with 60 mm in length and 0.9 mm in diameter. The basalt fibre was about 25.4 mm in length and 18 microns in diameter. The manufacturer provided tensile strength of steel was 1345 MPa. The tensile strength of basalt fibre was in the range of

Table 1 Mix proportions

	Series 1	Series 2	Series 3	Series 4
Constituents	Control	Steel FRC	Basalt FRC	Hybrid FRC
Water, Kg/m^3	225	225	225	225
Cement, Kg/m^3	562	562	562	562
Fine aggregate, Kg/m^3	668.85	668.85	668.85	668.85
Coarse aggregate (10mm), Kg/m^3	307.8	307.8	307.8	307.8
Coarse aggregate (20mm), Kg/m^3	615.77	615.77	615.77	615.77
Superplasticiser (mL)	100	100	100	100
Steel fibres (Vol. %)	-	0.5%	-	0.25%
Basalt fibres (Vol. %)	-	-	0.5%	0.25%

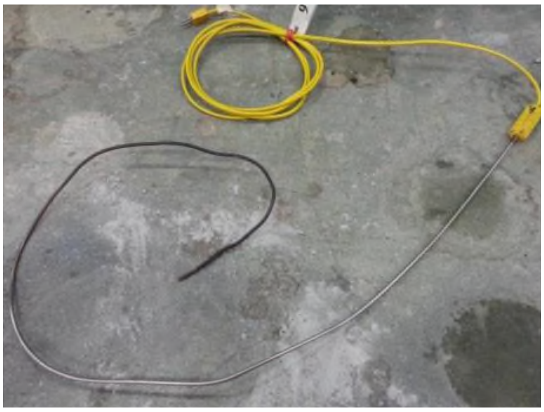

Fig. 1 Type *K* thermocouple

800-1200 MPa supplied by the manufacturer.

Total four series of concrete were considered in this study. The first series was the unreinforced ordinary Portland cement (OPC) concrete as control. The second and third series were steel and basalt FRC, where the volume fraction of each fibre was 0.5%. In the fourth series the hybridisation of steel and basalt fibres was considered. The total volume fraction of fibre was kept the same as second and third series. Detail mix proportions are shown in Table 1.

The mixing of control and fibre reinforced concretes was carried out in a pan mixer. First, the aggregates and cement were dry mixed for approximately 5 min, and then, water was slowly added into the mix and continued to mix for another 5 min. The fibres were then added gradually and mixed continually until uniform dispersion of fibres were observed in the mix. The cylinders were then filled with concretes and compacted on a vibrating table. The concrete cylinders were demoulded after 24 hours and stored in the curing tank where they were subjected to standard wet curing for 28 days. Before putting the specimens in the kiln, they were dried in an oven at 105°C for 24 hours to remove any free water from the concrete. This is to prevent the specimens from exploding in the kiln during the heating process, as a result of extremely high pore water pressure from the superheated water. To cast the concretes, steel cylindrical moulds of 200 mm in height and 100 mm in diameter were used. At least six cylinders were cast and test for each series and for each temperature. Some cylinders were modified in order to install 20 mm long and 2 mm diameter removable pins so that holes would be cast into the specimens for the thermocouples to be installed.

3. Heating regime

The kiln used to heat the cylinders was a locally manufactured kiln with a maximum temperature rating of 1200°C. It was a small capacity kiln capable of fitting a maximum of six cylinders at any one time. Details regarding the kiln can be found in Shaikh and Vimonsatit (2015). The heating rate of 8°C/min was applied as this was the maximum rate that could be achieved in the kiln. To monitor the temperatures, four 'type *K*' thermocouples shown in Fig. 1 were set up in different positions inside the kiln and in the cylinders (see Fig. 2). Two thermocouples were set up to monitor the air temperature inside the kiln. One was positioned 50mm from the top of the interior, and another was set 50mm from the bottom of the kiln. The other two thermocouples were inserted in to a sacrificial cylinder to monitor the core temperature of the sample. All four thermocouples were then connected to a data logger to monitor the temperatures inside the kiln and cylinder. Irrespective of the target temperature, the testing method remained the same throughout. Oven-dried samples were put into the kiln and immediately exposed to an 8°C/min heating rate. This heating rate was continued until the ambient temperatures inside the kiln reached the target temperature. At this point, the target temperature was maintained, and the concrete was held in the kiln for a further 2 hours.

The rate of temperature increase in the kiln and in the cylinder is shown in Fig. 3. The top two lines are for the thermocouples measuring the air temperature inside the kiln, while the bottom two lines are the readings for the concrete cylinder. As can be seen in the figure, there is some difference between the core temperature of concrete cylinder and the air temperature inside the kiln, particularly for 400°C temperature profile. This is due to the heat capacity of the concrete specimens and the rate at which they are able to absorb heat. However, the difference between kiln temperature and cylinder at 800°C gradually reduced.

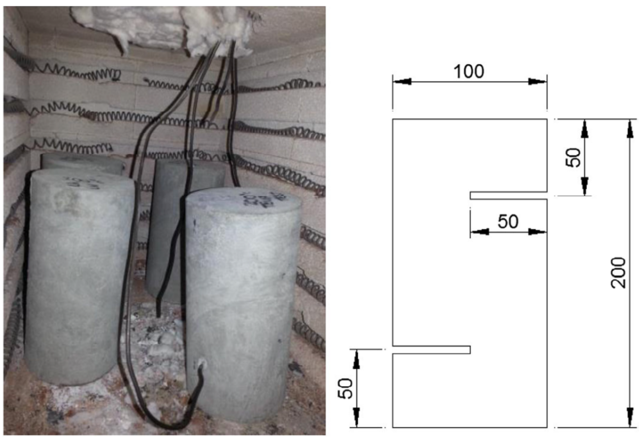

Fig. 2 Location of thermocouples inside the kiln (left) and in concrete cylinder (right)

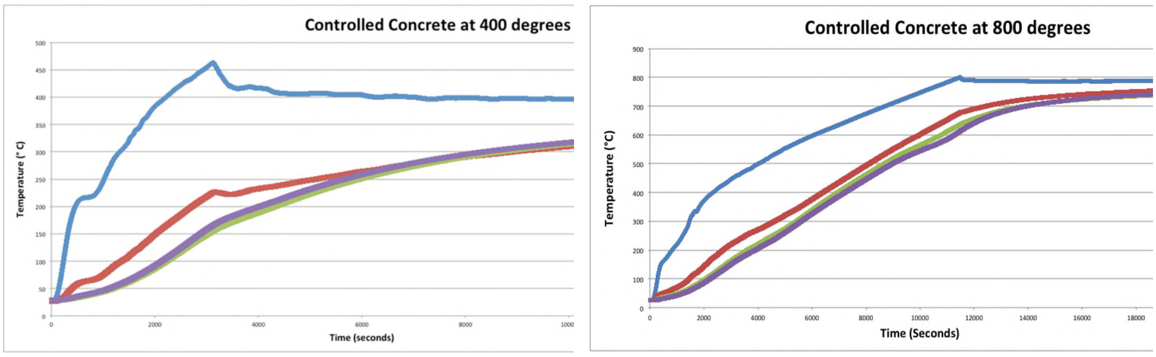

(a) (b)

Fig. 3 Temperature profiles in kiln and specimen for target elevated temperatures of (a) 400°C and (b) 800°C

Table 2 Compressive strengths of all concretes including standard deviation (SD) and coefficient of variation (COV)

	Ambient			400°C			800°C		
	Compressive Strength (MPa)	SD	COV (%)	Compressive Strength (MPa)	SD	COV (%)	Compressive Strength (MPa)	SD	COV (%)
Control	42.6	5.4	12.6	31.3	3.3	10.5	11.1	1.6	14.1
Steel FRC	51.2	4.2	8.3	37.8	1.1	2.9	14.5	1.5	10.4
Basalt FRC	38.5	4	10.5	20.9	2.4	11.4	5.3	0.6	12.2
Hybrid FRC	47.8	2.8	5.9	31.9	2.6	8.1	10.6	0.7	6.5

4. Results and discussion

4.1 Compressive strength

Table 2 summarises the measured compressive strength of all four types of concretes with their standard deviation (SD) and coefficient of variation (COV). The measured compressive strengths of all four types of concretes at ambient condition are shown in Fig. 4(a). It can be seen about 12% increase in the compressive strength of steel-FRC compared to control concrete, which is reasonable as the addition of fibres hardly affect the compressive strength of concrete (Ezeldin and Balaguru 1992, Fanella and Naaman 1985). The slightly higher compressive strength in steel-FRC can be attributed to the bringing of micro-cracks by the steel fibres, which increased the ultimate failure load in compression. On the other hand, the basalt-FRC shows an opposite trend, where about 10% reduction in compressive strength is observed compared to the control concrete. Similar results are also reported by Dias and Thaumaturgo (2005), Borhan (2013) in the case of basalt fibre reinforced concrete (0.5% (by vol.) basalt fibre). While the reason for reduction in compressive strength is not exactly clear, but the poor interface of basalt fibre with cement matrix as well as increase in porosity due to addition of basalt fibres in cement paste reported by Jiang *et al*. (2014) could be the contributing factors. However, when hybrid combination of both steel and basalt fibres are used, the negative effect of basalt fibre in the compressive strength is overcome with slight increase in compressive strength compared to control concrete.

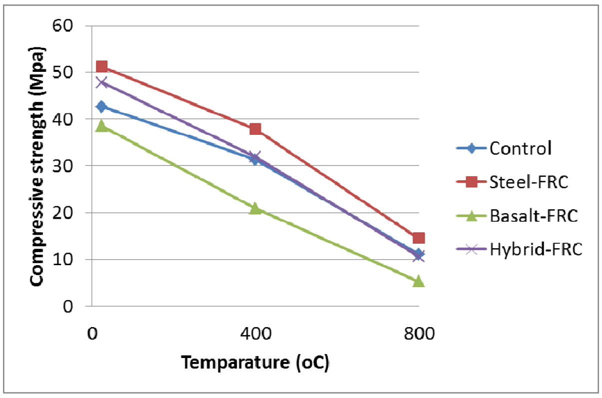

(a)

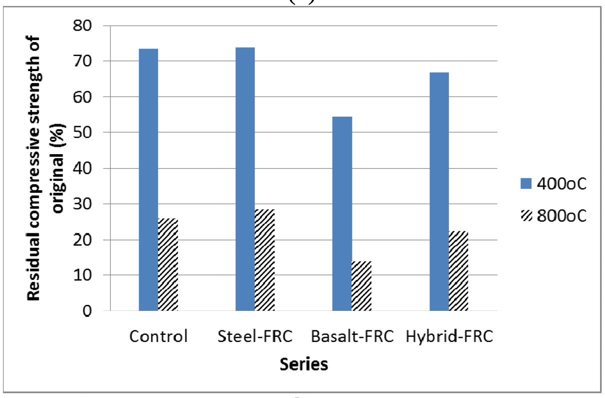

(b)

Fig. 4 Effects of elevated temperatures on the compressive strength of four types of concretes

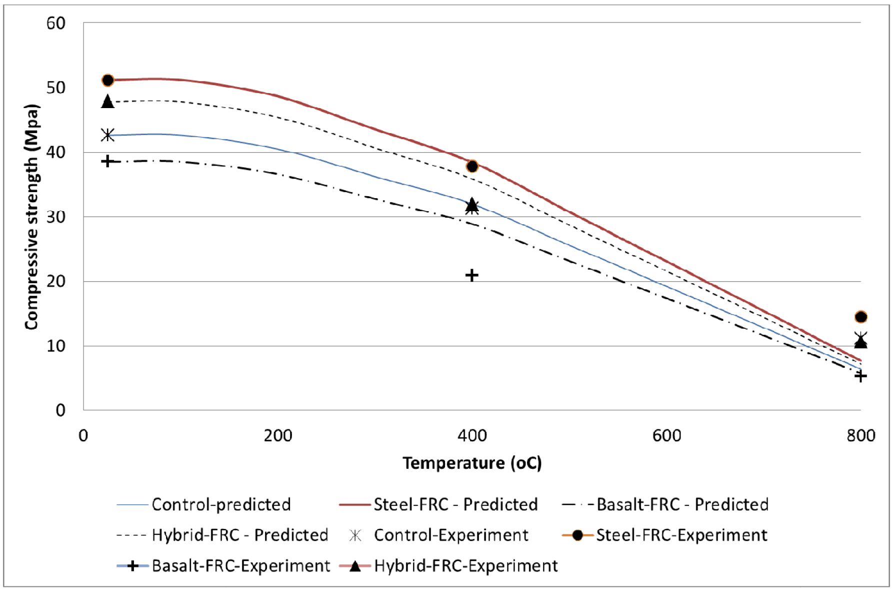

Fig. 5 Comparison of experimentally measured compressive strengths at elevated temperatures with those predicted by Eurocode EN1994-1-2:2003

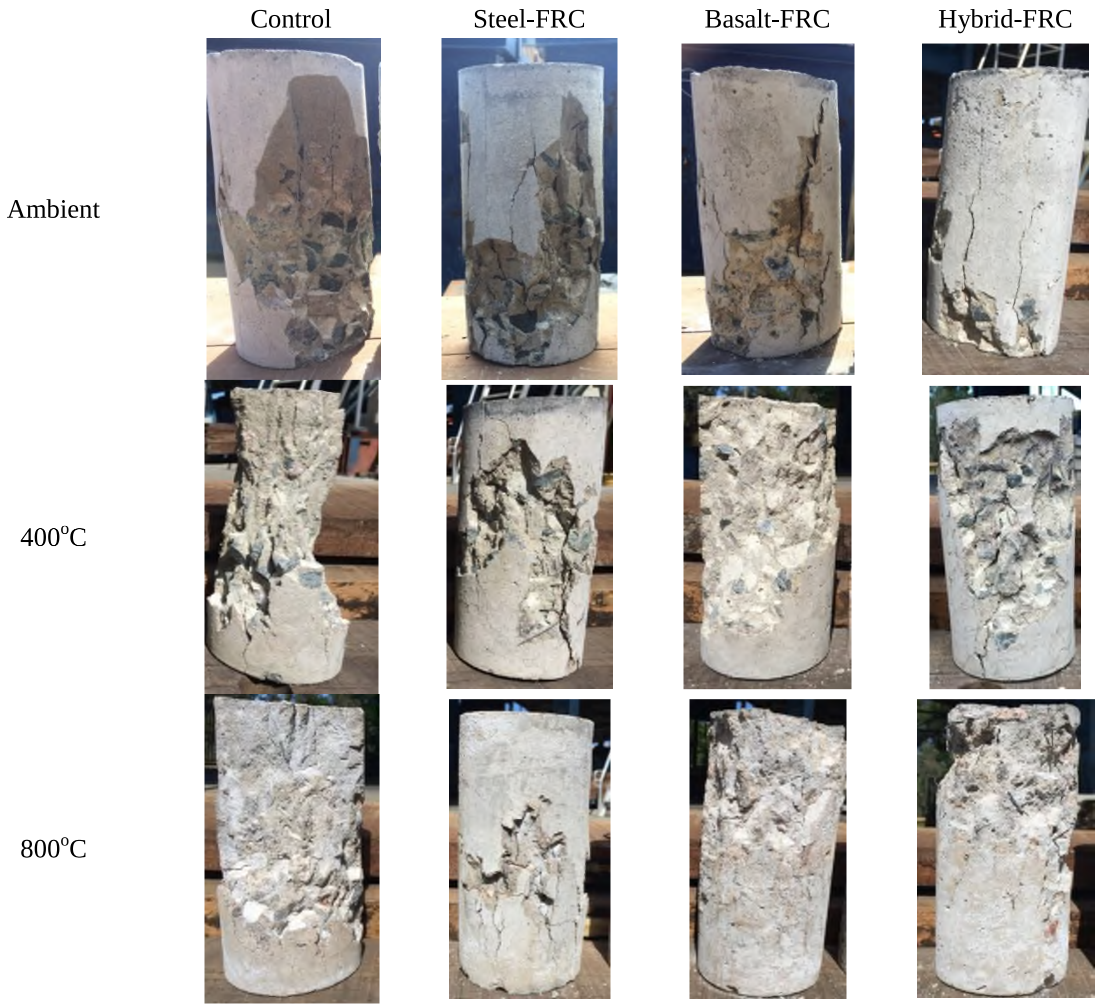

Fig. 6 Failure modes of control, Steel-FRC, basalt-FRC and hybrid-FRC concretes at compression after exposure to 400 and 800°C temperatures

The effects of elevated temperatures of 400 °C and 800°C on the compressive strength of three types of fibre reinforced concretes as well as control concrete are also shown in Fig. 4(a). It can be seen that the compressive strength is decreased in all four types of concretes at elevated temperatures and the rates of decrease of compressive strength of all concretes are very similar. In Fig. 4(b) the residual compressive strengths of all four concretes at 400°C and 800°C temperatures are shown and it can be seen that the steel-FRC performed better than the other two FRCs when compared with control concrete. The steel-FRC showed slightly higher residual compressive strength at both temperatures compared to the control. On the other hand, the basalt-FRC exhibited the lowest residual capacity of about 52% and 15% of original at 400°C and 800°C, respectively. Both steel-FRC and basalt-FRP exhibited much higher residual capacity at 400°C than 800°C and can be attributed to the higher thermal stability of both fibres at 400°C. However, the inferior performance of basalt-FRC than the steel-FRC could be due to very low tensile strength of single

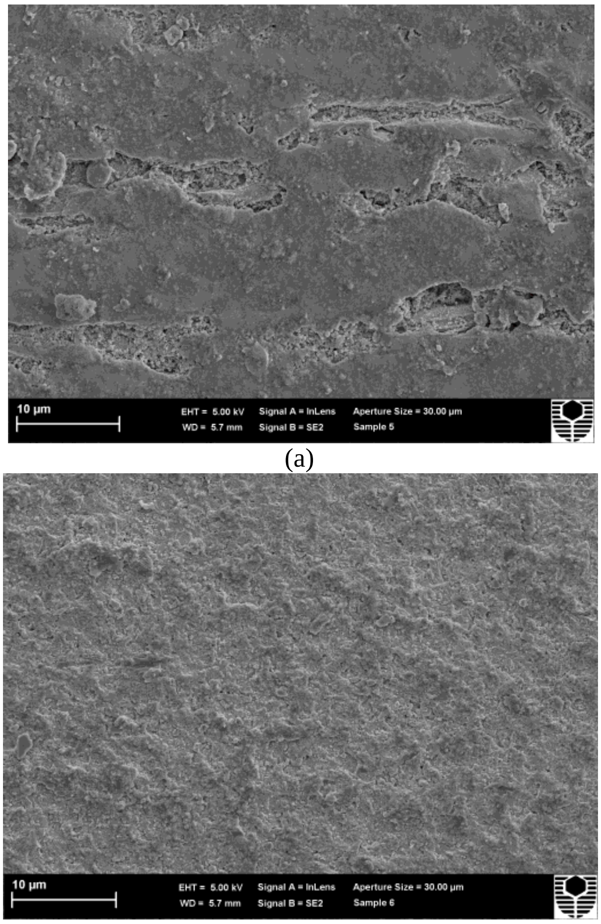

(a)

(b)

Fig. 7 SEM images of steel fibre surface at 400 °C (left) and 800 °C (right) temperatures. (2000X magnification)

basalt filament compared to the tensile strength of single steel fibre, poor basalt-matrix interface (Jiang *et al*. 2014) and the shorter length of basalt fibre than the steel fibre.

4.2 Comparison of results with prediction

The measured compressive strengths of above FRCs at 400°C and 800°C are also compared with those predicted by the existing model (EN1994, 2005) to evaluate its applicability in the prediction of compressive strength of FRCs at elevated temperatures. Fig. 5 shows the comparison of measured compressive strength of fibre reinforced concretes and control concrete at 400^{o}C and 800°C with that predicted by the model. It can be seen in the figure. that the measured compressive strengths of control concrete at 400°C and 800°C are very close to the predicted values. In the case of steel-FRC, the Eurocode model predicted the measured compressive strength at 400°C with good accuracy. However, at 800°C the model underestimated the measured value. An opposite scenario can be seen in the case of basalt-FRC where the model overestimated the

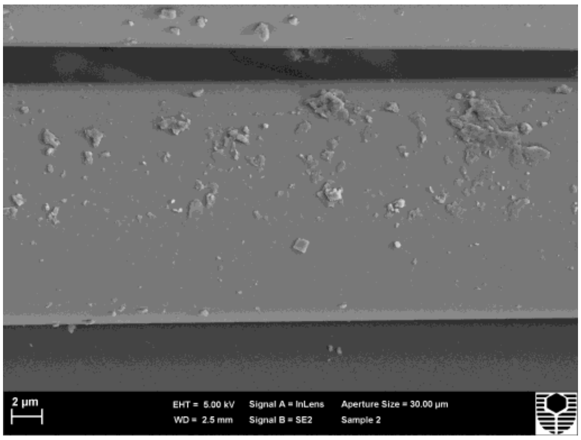

(a)

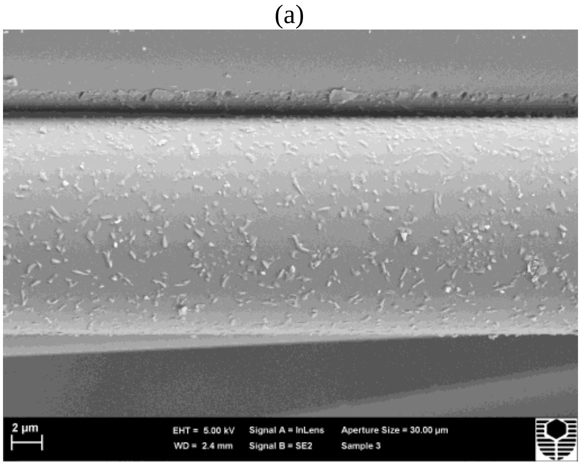

(b)

Fig. 8 SEM images of basalt fibre surface at 400^{o}C (left) and 800^{o}C (right) temperatures. (3000X magnification)

measured strength at 400^{o}C. However, in the case of hybrid-FRC the model also predicted the measured strengths with reasonable accuracy. In the absence of any model for the FRCs, more research is needed to confirm the applicability of the Eurocode EN1994 (2005) to predict the compressive strength of FRCs at various elevated temperatures.

4.3 Failure behaviour

The effects of steel and basalt fibres and their hybrid effects on the failure behaviour of concrete after exposure to 400 and 800°C temperatures are also evaluated and are shown in Fig. 6. It can be seen that the unreinforced control concrete exhibited significant spalling of concrete in compression at both temperatures. However, at the same temperature, the steel-FRC exhibited better behaviour with significantly less spalling presumably due to the crack-bridging of steel fibres in the concrete. On the other hand, consistent with compressive strength results, the basalt-FRC showed much higher spalling at both temperatures than steel-FRC, however, much less than control concrete. The hybrid-FRC also exhibited better behaviour in terms of less area of spalling than the basalt-FRC. Nevertheless, all three FRCs exhibited better spalling resistance than the control concrete at both temperatures.

4.4 Microstructural observation

The physical changes of both steel and basalt fibres after exposure to elevated temperatures of 400 and 800°C are also examined using scanning electron microscope (SEM) analysis technique. Figs. 7 and 8 show the SEM images of the surface of both fibres. It can be seen that at 400°C fractures on top layer of the steel fibre surface are formed (Fig. 7(a)) and at 800^{o}C this surface layer is completely peeled off exposed a rough surface (Fig. 7(b)). On the other hand, at 400°C the outer layer of basalt fibre is restructure and mineral crystals are formed as shown in Fig. 8(a). As the temperature rose to 800°C more crystals are formed and grown out of basalt surface as shown in Fig. 8(b). These recrystallization can be interpreted as the mineral phase Plagioclase, because Plagioclase melts at 800°C and below whereas potential basalt mineral phases such as, Olivines and Pyroxens display higher melting points. Stockmann *et al*. (2014) recently observed that the Calcite, which presents in cement, is the slowest to crystallize on basalt glass out of six different basalt mineral phases. It is therefore plausible that the poor interface of basalt fibre in the cement matrix is due to the weak or non-bonding nature of the connection between basaltic glass and the cement matrix as large surface area of basalt fibres were present in the cement paste. This lack of adhesion consequently resulted in a substantial reduction in the measured compressive strength in this study as well as observed by others (Ma *et al*. 2010, Ayub *et al*. 2014).

5. Conclusions

Based on limited experiments on the effect of elevated temperatures on the compressive strengths and failure behaviour of different fibre reinforced concretes, the following conclusions can be drawn

1. The residual compressive strength of steel fibre reinforced concrete is higher than the control unreinforced concrete at both elevated temperatures. The basalt fibre reinforced concrete, on the other hand, exhibited lower residual compressive strength than the control unreinforced concrete. The use of hybrid steel-basalt fibre reinforcement recovered this deficiency of basalt fibre reinforced concrete, however, still slightly lower than the control concrete and steel fibre reinforced concrete.

2. The existing Eurocode EN1994 (2003) predicted the compressive strengths of fibre reinforced concretes with reasonable accuracy. However, more research need to be conducted as in some instances (e.g., in the case of steel-FRC at 800^{o}C and basalt-FRC at 400^{o}C) the over and under estimated results are obtained.

3. The addition of both steel and basalt fibres reduced the spalling and explosive failure of fibres reinforced concretes under compressive load oppose to spalling in deeper regions of control concrete.

4. Microscopic observation of steel and basalt fibres surfaces after exposure to elevated temperatures showed peeling of thin layer from steel surface at 800^{o}C, whereas in the case of basalt fibre formation of Plagioclase mineral crystals on the surface are observed at elevated temperatures. This study also observed that the poor performance of basalt fibre reinforced concrete at elevated temperatures is due to poor bond of basalt fibre with cement matrix despite

their higher fire resistance.

Acknowledgements

Authors gratefully acknowledge BOSFA and Basalt fibre technology for donating steel and basalt fibres, respectively in this study.

References

Ali, F.A., Connolly, R. and Sullivan, P.J.E. (1996), "Spalling of high strength concrete at elevated temperatures", *J. Appl. Fire Sci*., **6**(1), 3-14.

Ayub, T., Shafiq, N. and Nuruddin, M.F. (2014), "Mechanival properties of high performance concrete reinforced with basalt fibres", *Procedia Eng*., **77**, 131-139.

Borhan, T.M. (2013), "Thermal and mechanical properties of basalt fibre reinforced concrete", *Int. scholarly Sci. Res. Innov*., **7**(4), 712-715.

Chen, B. and Liu, J. (2004), "Residual strength of hybrid-fiber-reinforced high-strength concrete after exposure to high temperatures", *Cement Concrete Res.*, **34**(6), 1065-1069.

Dias, D.P. and Thaumaturgo, C. (2005), "Fracture toughness of geopolymeric concretes reinforced with basalt fibers", *Cement Concrete Comp*., **27**(1), 49-54.

Dugenci, O., Haktanir, T. and Altun, F. (2015), "Experimental research for the effect of high temperature on the mechanical properties of steel fibre reinforced concrete", *Constr. Build. Mater*. **75**, 82-88.

EN 1994-1-2 (2003), *Design of composite steel and concrete structures-part 1-2: general rules* - structural fire design, Eurocodes.

Ezeldin, A.S. and Balaguru, P.N. (1992), "Normal-and high-strength fiber-reinforced concrete under compression", *J. Mater. Civil Eng.*, **4**(4), 415-429.

Fanella, D.A. and Naaman, A.E. (1985), "Stress-strain properties of fiber reinforced mortar in compression", *ACI J.*, **82**(4), 475-483.

Jiang, C., Fan, K., Wu, F. and Chen, D. (2014), "Experimental study on the mechanical properties and microstructure of chopped basalt fibre reinforced concrete", *Mater. Des.*, **58**, 187-193.

Kim, J. and Lee, G.P. (2015), "Evaluation of mechanical properties of steel-fibre-reinforced concrete exposed to high temperatures by double-punch test", *Constr. Build. Mater.*, **79**, 182-191.

Ma, J., Qiu, X., Cheng, L. and Wang, Y. (2010), "Experimental research on the fundamental mechanical properties of presoaked basalt fibre concrete", *Proceedings of the 5th International Conference on FRP Composites in Civil Engineering*, Beijing, China.

Poon, C.S., Shui, Z.H. and Lam, L. (2004), "Compressive behavior of fiber reinforced high-performance concrete subjected to elevated temperatures", *Cement Concrete Res.*, **34**(12), 2215-2222.

Shaikh, F.U.A. and Vimonsatit, V. (2015), "Compressive strength of fly-ash-based geopolymer concrete at elevated temperatures", *Fire Mater.*, **39**(2), 174-188.

Stockmann, G.J., Wolff-Boenisch, D., Bovet, N., Gislason, S.R. and Oelkers, E.H. (2014), "The role of silicate surfaces on calcite precipitation kinetics", *Geochimica et Cosmochimica Acta*, **135**, 231-250.

Suhaendi, S.L. and Horiguchi, T. (2006), "Effect of short fibers on residual permeability and mechanical properties of hybrid fibre reinforced high strength concrete after heat exposition", *Cement Concrete Res.*, **36**(9), 1672-1678.

Wetzig, V. (2002), "The fire resistance of various types or air placed concrete", *4th International Symposium on Sprayed Concrete*, 352, Davos, Switzerland, September.

JK